POSITIVE EFFECTS OF FRONT SURFACE FIELD IN HIGH-EFFICIENCY BACK-CONTACT BACK-JUNCTION *N-TYPE* SILICON SOLAR CELLS

Filip Granek, Martin Hermle, Christian Reichel, Andreas Grohe, Oliver Schultz-Wittmann*, Stefan Glunz
Fraunhofer Institute for Solar Energy Systems, Heidenhofstr. 2, D-79110 Freiburg, Germany
Phone: +49-761-4588-5287; Fax: +49-761-4588-9250; email: filip.granek@ise.fraunhofer.de
*now with Solexel Inc., California

ABSTRACT

The role of the phosphorus-doped front surface field (FSF) in *n-type* back-contact back-junction silicon solar cells was analyzed. The FSF improves the quality of the front surface passivation and enables very high efficiencies even for the cells with higher front surface recombination velocity. The stability of the front surface passivation using the FSF with respect to UV-light was analyzed by measurements of lifetime samples. Application of the FSF significantly improves the UV-light stability. The surface saturation current density (J_{0e}) of the textured lifetime samples without FSF increased form 30 fA/cm^2 to almost 450 fA/cm^2 after 55 hours of UV-light exposure. J_{0e} of the samples with FSF showed only a marginal increase from 30 to 35 fA/cm^2. An additional positive effect of the FSF is the reduction of the lateral resistance losses. These losses are caused by a significant increase of the pitch on the rear cell side, when only low-cost structuring technologies (screen-printing and laser processing) are applied. An experimental study showed that the FSF strongly improved the fill factors of the cells with large pitches. Two-dimensional device simulations revealed that the FSF significantly contributes to the lateral transport of the majority carrier's current. The best cell efficiency of 21.3 % was obtained for the solar cell with a 1 Ω cm specific base resistivity and a front surface field with a sheet resistance of 148 Ω/sq.

INTRODUCTION

The back-contacted and back-side collecting silicon solar cell design represents a very attractive cell structure with high efficiency potential in the mass production. Sunpower Corp. demonstrated recently for this cell type efficiencies exceeding 22 % in its production lines [1]. One of the most important features of the back-contacted and back-junction (BC-BJ) cell structure [1,2] is the presence of the front surface field (FSF). In this paper we discuss three different positive effects of the FSF. First, we will have a look at the passivation quality of the front side passivation using the FSF, since it is one of the most critical parameters to the performance of a BC-BJ cell. Second, the stability of the front side passivation with respect to the UV-light is analyzed for samples with and without the FSF. Third, the effect of the reduction of the lateral resistance losses due to the increased lateral current transport via the FSF is discussed. This effect is significant only if the cell pitch (see Fig. 1) is large, due to the use of industrially applicable structuring technologies such as ink-jetting and screen-printing of resist masks or laser processing. Then the FSF not only improves the front side passivation and the passivation stability, but also reduces the lateral resistance for the majority carriers.

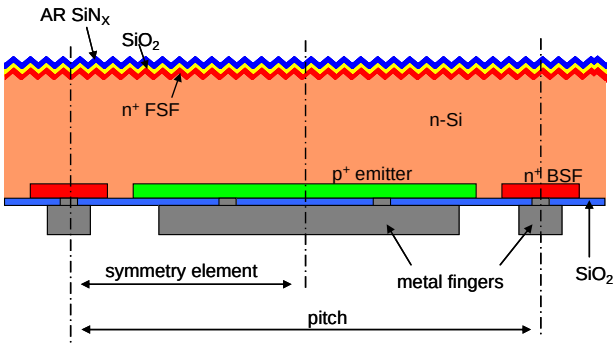

Figure 1. Schematic cross-section of the *n-type* high-efficiency back-contact back-junction silicon solar cell processed at Fraunhofer ISE (sketch is not to scale). Pitch and the symmetry element used for two-dimensional device simulations are shown.

PASSIVATION OF THE FRONT SIDE OF THE BACK-JUNCTION CELLS WITH FSF

In the solar cell most of the photo-generation occurs at the front side, where the light-generated carriers can easily be lost by recombining at a poorly passivated surface instead of reaching the *p-n* junction at the rear surface. Thus, an excellent front surface passivation is one of the critical factors influencing the efficiency of the back-junction cell type. FSF is well-known to improve the front side passivation [3, 4]. In Fig. 2 the PC1D [5] simulations of the influence of the front surface recombination velocity ($S_{0,front}$) on the back-junction back-contact cell performance is shown. Efficiency of the back-junction cells with a FSF is high in a very wide range of $S_{0,front}$. In contrast, the efficiency of the cells without the FSF decreases rapidly as the $S_{0,front}$ increases. Thus, the application of the FSF enables a very good cell

performance even for non-ideal surface passivation. The ability of the FSF to improve the effective front side passivation of the cells with higher $S_{0,front}$ is especially important for the manufacturing of the high-efficiency cells in industrial processing environment, where perfect $S_{0,front}$ values are more difficult to obtain than in a laboratory environment.

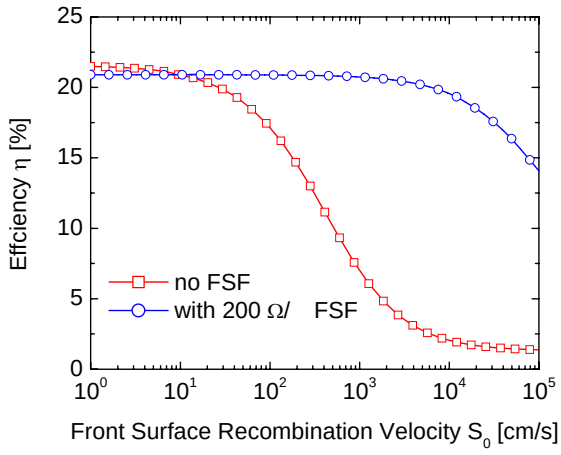

Figure 2. Influence of the front surface recombination velocity ($S_{0,front}$) on the efficiency of back-junction *n-type* Si solar cells with and without the FSF (one-dimensional PC1D [5] simulations).

UV-STABILITY OF FRONT SURFACE PASSIVATION

Another positive effect of the FSF is a significant improvement of the UV-light stability of the front side passivation, which is very important for the long term operation of the solar cells. The UV-stability of the front surface passivation with and without FSF was examined by exposing the n^+nn^+ lifetime samples to UV-light (Xenon lamp) at one sun light intensity and a temperature of 50 °C. The tested samples were not covered with module glass during the exposure. The symmetrical lifetime samples were textured with random pyramids and the both surfaces were passivated with a thin thermal SiO_2 layer and an antireflection-SiN_X coating. The samples were annealed in a forming gas atmosphere prior to the exposure test.

Results of the exposure tests are shown in Fig. 3. Lifetime of samples without FSF degrades significantly already after the first few hours of exposure. Surface saturation current density J_{0e} was determined after each exposure step. Details of the determination of J_{0e} can be found in Ref. 6. For the samples without the FSF, J_{0e} increases from initial value of ~30 fA/cm^2 to almost 450 fA/cm^2 after 55 hours of UV-light exposure. Such a high increase of J_{0e}, which corresponds to $S_{0,front}$ of ~140 cm/s, will lead to a significant cell performance degradation (see Fig. 2). Samples with FSF show no significant degradation. J_{0e} increases from ~30 to 35 fA/cm^2 in the case of a 148 Ω/sq FSF diffusion. This proves that passivation using a FSF is stable and therefore appropriate for industrial applications in contrast to unstable passivation without FSF. Similar results were already obtained by Gruenbaum *et al*. [7].

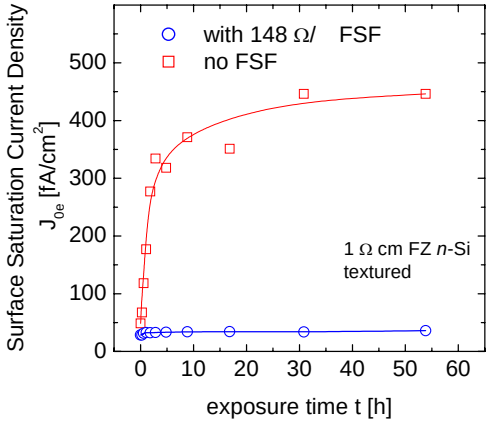

Figure 3. Passivation stability of textured n^+nn^+ lifetime samples with and without FSF during 55 hours of exposure to UV-light. Lines are guides-to-the-eye.

IMPLICATIONS OF THE USE OF LOW-COST STRUCTURING TECHNOLOGIES

Back-contact back-junction solar cells were processed by our group without the use of photolithography. Application of low-cost structuring technologies, such as screen-printing and laser processing, leads to the reduction of the resolution and positioning accuracy. This results in the *p-n* pitches in the range of millimeters. Thus, the pitch on the rear side increases by a factor of 20 to 50 when comparing to the cells processed with the use of photolithography, e.g. point-contact solar cells of Sinton e*t al.* [8] which had a pitch of 45 µm. With the large lateral dimensions of the pitch, the majority carriers current needs to flow laterally distances in the range of millimeters before reaching the base contacts. Lateral transport of the majority carriers is causing significant series resistance losses due to its larger distances. When a highly doped FSF layer is present, the lateral transport of the electrons can be enhanced. This additional positive effect of the FSF is sketched in Fig. 4.

In order to experimentally investigate the influence of the FSF on the lateral majority current transport, a set of solar cells with different pitches were processed. Back-contact back-junction *n-type* silicon solar cells with pitches of 1.3, 1.8, 2.2 and 3.5 mm were fabricated (see Tab I). The pitch and the base and emitter width had to be selected, so that the resolution and positioning accuracy of the cell geometry can be done using low-cost masking steps such as screen-printing and laser ablation. The width of the emitter area (p^+) was varied in the range of 700 - 2900 µm in order to investigate the lateral current transport in the base and in the FSF. The base width was fixed at 600 µm for all investigated pitches.

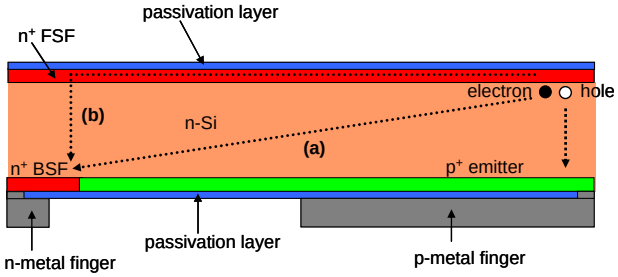

Figure 4. Schematic drawing of the effect of the enhanced lateral current transport of the majority carriers via the front surface field (symmetry element of the cell is shown). For simplicity the front side texture is not shown. The lateral current transport through the FSF (b) can be seen as an additional transport path to the base lateral resistance (a).

Table I. Geometry parameters of the rear side of the back-contacted solar cells with different pitches.

Structure	A	B	C	D
Emitter [µm]	700	1200	1600	2900
Base [µm]	600	600	600	600
Pitch [µm]	1300	1800	2200	3500
Emitter fraction [%]	54	67	73	83

A schematic cross-section of the BC-BJ *n-type* Si solar cell structure analyzed in this paper is shown in Fig. 1. The 2 x 2 cm^2 cells were fabricated from *n*-type, 200 µm thick float-zone (FZ) silicon wafers. Specific base resistivities of 1 and 8 Ω cm were chosen. The front side is textured with random pyramids and passivated with a lightly doped ($N_{peak} = 5\times10^{18}$ cm^{-3}) and deep diffused (1.4 µm) phosphorus front surface field (FSF) diffusion with the sheet resistance of 148 Ω/sq. Our investigations of the surface passivation quality of different FSF diffusion profiles were presented in Ref 6. The front surface was then passivated with a thin thermally grown silicon dioxide layer and a PECVD silicon nitride (SiN_x) antireflection coating. Both emitter p^+ and back surface field n^+ diffusions are separated by an undiffused gap. The rear cell surface is passivated with silicon dioxide. Metal fingers are contacted to the diffused regions through local openings in dielectric layer. The cells were annealed in forming gas atmosphere. Prior to measurements, the cells were removed from the host wafer by the means of laser cutting with an edge distance of 500 µm from active cell area. Next to the solar cells processing, two-dimensional device simulations using a numerical device simulation program Sentaurus Device™ [9] were performed.

IMPACT OF THE FSF ON THE FILL FACTOR AND THE LATERAL CURRENT TRANSPORT

The fill factors of the processed cells with different pitches are shown in the Fig. 5. As one would expect, the FF decreases as the pitch increases due to increased lateral resistance in base. For the cells with specific base resistivity of 1 Ω cm and with the FSF, the increase of pitch from 1.3 to 3.5 mm results in a FF drop of about 1 % absolute. The FF of the 1 Ω cm cells without the FSF is around 1 $\%_{abs}$ lower than the FF of the cells with the FSF. The impact of the FSF on the lateral resistance losses and on the FF is even more pronounced for the cells with the 8 Ω cm specific base resistance. Here much lower fill factors were obtained. For the pitch of 1.3 mm a maximum FF of 79 % and 78 % for cells with and without FSF respectively was measured. When reaching the largest pitch of 3.5 mm, the FF dropped to 76 % for cells with FSF and to 63 % for cells without FSF. Thus, the increase of the pitch form 1.3 to 3.5 mm caused a FF drop by 3 $\%_{abs}$ for the cells with FSF, and for the cells without the FSF the FF dropped drastically by 13 $\%_{abs}$.

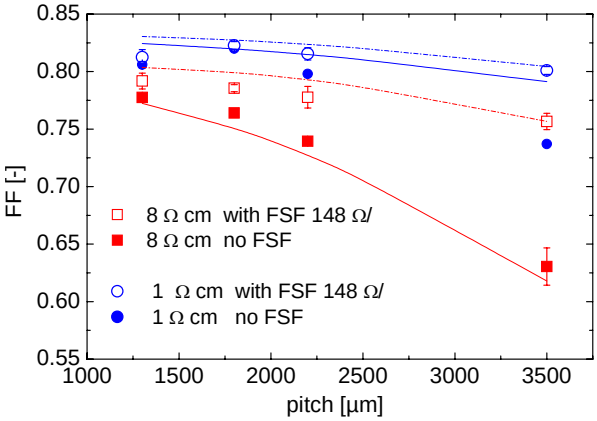

Figure 5. Fill factor of the processed cells and two-dimensional numerical simulations as a function of the pitch for two different base resistivities. Results for the cells with (ρ_{sheet} = 148 Ω/sq) and without FSF diffusion are shown. The data points represent a mean value of the experimental results. Lines represent the 2D simulation results.

Next to the measured fill factor values, also the 2D simulations are shown in Fig. 5. A good agreement between the experimental and 2D simulation results can be observed. These results clearly demonstrate that the FSF significantly reduces the series resistance losses and thus improves FF in comparison to cells without FSF. The effect of enhanced current transport in FSF is stronger for larger pitches, where the base lateral resistance dominates the resistance losses of the cell. Moreover, the additional impact of the FSF is, as expected, a function of the base doping. For higher base resistivity (8 Ω cm) and large pitch distance (3.5 mm) the FF of the cells with FSF is up to 13 $\%_{abs}$ higher than the FF of the cells without the FSF. In this experiment the best cell efficiency of 21.3 % (designated cell area measurement) was obtained for a base resistivity of 1 Ω cm and a pitch of 1.8 mm. Optimum pitch was found to be 1.8 to 2.2 mm. This optimum represents the best trade-off between emitter coverage on the rear side and series resistance losses due to the increased lateral distances.

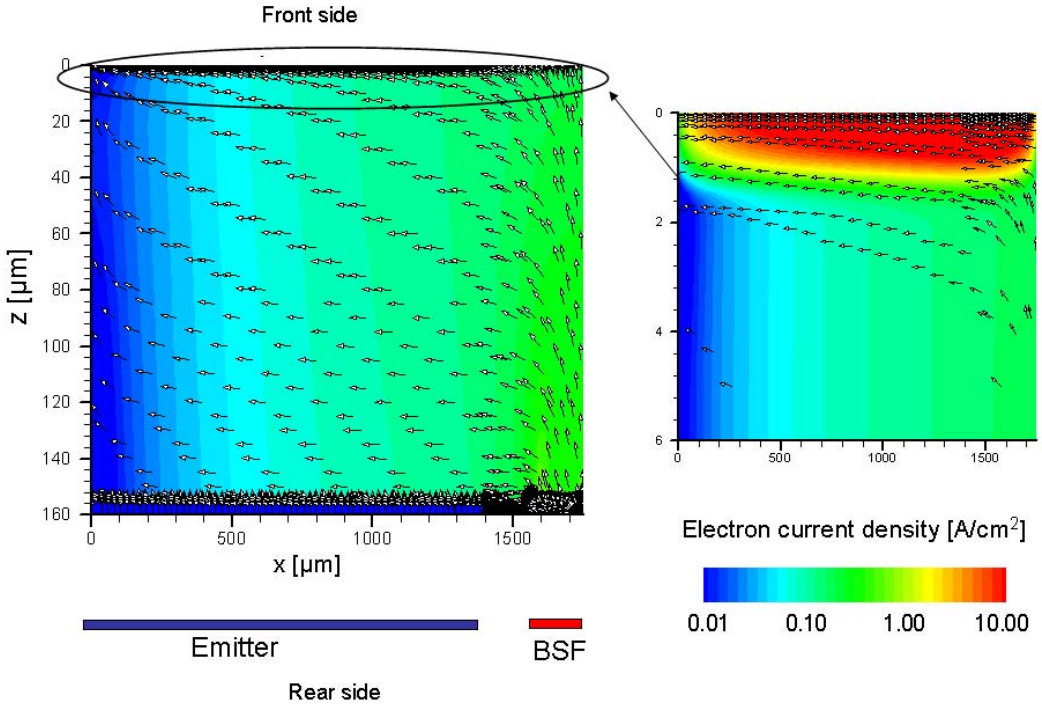

Figure 6. Two-dimensional modelling results of the lateral and vertical electron current transport in the *n-type* back-contact back-junction solar cell structure with a base resistivity of 8 Ω cm and a pitch distance of 3.5 mm. The symmetry element of the solar cell is shown. The arrows show the technical current direction of the electron current (opposite direction of the particle flow) at V_{MPP} of a cell with front surface field (ρ_{sheet} = 148 Ω/sq).

The two-dimensional simulations of the majority carrier's current transport are shown in Fig. 6. Here the extreme case of the largest pitch of 3.5 mm was analyzed. Increased electron current density in the front surface field area is shown in detail (right side). The electron current density in the FSF area is around two orders of magnitude higher than in the base. This simulation shows that the lateral electron current transport not only takes place in the base, but also in the FSF. The electrons, which were photo-generated at the front cell side in the first few micrometers of the wafer, take advantage of the lateral transport in the FSF. Thus, the lateral base resistance is strongly reduced and the FSF improves the fill factor of the cell.

CONCLUSIONS

The different functions of the front surface field in the *n-type* back-contact back-junction solar cells processed with the use of industrially relevant structuring technologies such as screen-printing and laser processing were discussed. The FSF improves the front surface passivation of the cells with poor $S_{0,front}$, enabling high efficiencies even without perfectly passivated front surfaces. Second, the application of the FSF significantly improves the stability of the front surface passivation with respect to the UV-light illumination. Thus, the efficiency of the cells with the FSF will be maintained during the long-term operation in the solar module. Third, the FSF plays an important role in the lateral transport of the majority carriers current. This function of the FSF is especially pronounced, when lateral dimensions of the cell are large, due to the application of the low-cost structuring technologies. Here the FSF reduces the lateral resistance losses and improves the fill factor of the cells. This function of the FSF could be demonstrated by experiments and two-dimensional device simulations. According to the two-dimensional simulations of the electron current transport, the electron current density in the FSF is around two orders of magnitude higher than in the base of the solar cell. Finally, a cell efficiency of 21.3 % for the cells processed with the low-cost masking with a front surface diffusion of 148 Ω/sq could be demonstrated.

ACKNOWLEDGMENTS

The authors thank A. Leimenstoll, C. Harmel and A. Herbolzheimer for the solar cell processing, E. Schäffer for the measurements. Fruitful co-operation and many valuable discussions with our partners at Q-Cells AG and N.-P. Harder from the ISFH are gratefully acknowledged. This work was supported by the German Federal Ministry for the Environment, Nature Conservation and Nuclear Safety under contact no. 0329988 (QUEBEC project).

REFERENCES

[1] D. De Ceuster, P. Cousins, D. Rose, D. Vicente, P. Tipones, and W. Mulligan, "Low Cost, high volume production of >22% efficiency silicon solar cells," Proceedings of the 22nd European Photovoltaic Solar Energy Conference, Milan, Italy, 2007, pp. 816-819.

[2] D. Huljic, T. Zerres, A. Mohr, K. v. Maydell, K. Petter, J. W. Müller, H. Feist, N.-P. Harder, P. Engelhart, T. Brendemühl, R. Grischke, R. Meyer, R. Brendel, F. Granek, A. Grohe, M. Hermle, O. Schultz, and S. W. Glunz, "Development of a 21 % back-contact monocrystalline silicon solar cell for large-scale production," Proceedings of the 21st European Photovoltaic Solar Energy Conference, Dresden, Germany, 2006, pp.765-768.

[3] R. R. King, R. A. Sinton, and R. M. Swanson, "Front and back surface fields for point-contact solar cells," Proceedings of the 20th IEEE Photovoltaic Specialists Conference, Las Vegas, Nevada, USA, 1988, pp. 538-544.

[4] M. Hermle, F. Granek, O. Schultz, and S. W. Glunz, "Analyzing the effects of front-surface fields on back-junction silicon solar cells using the charge-collection probability and the reciprocity theorem," *Journal of Applied Physics*, vol. **103**, 2008, pp. 054507/1-7.

[5] D. A. Clugston and P. A. Basore, "PC1D version 5: 32-bit solar cell modeling on personal computers," Proceedings of the 26th IEEE Photovoltaic Specialists Conference, Anaheim, California, USA, 1997, pp. 207-210.

[6] F. Granek, C. Reichel, M. Hermle, D. M. Huljic, O. Schultz, and S. W. Glunz, "Front surface passivation of n-type high-efficiency back-junction silicon solar cells using front surface field," Proceedings of the 22nd European Photovoltaic Solar Energy Conference Milan, Italy, 2007, pp. 1454-1457.

[7] P. E. Gruenbaum, R. A. Sinton, and R. M. Swanson, "Stability problems in point contact solar cells," Proceedings of the 20th IEEE Photovoltaic Specialists Conference, Las Vegas, Nevada, USA, 1988, pp. 423-428.

[8] R. A. Sinton, Y. Kwark, P. Gruenbaum, and R. M. Swanson, "Silicon point contact concentrator solar cells," Proceedings of the 18th IEEE Photovoltaic Specialists Conference, Las Vegas, Nevada, USA, 1985, pp. 61-65.

[9] Synopsys Zurich, Switzerland, TCAD SDEVICE Manual (2007) Release: Z-2007.03 www.synopsys.com